Low-Rate Farrow Structure with Discrete-Lowpass and Polynomial Support for Audio Resampling

Aleksej Chinaev, Philipp Thüne and Gerald Enzner
Institute of Communication Acoustics, Ruhr-Universität Bochum, 44780 Bochum, Germany
Email: {aleksej.chinaev, philipp.thuene, gerald.enzner}@rub.de

***Abstract*—Arbitrary sampling rate conversion (ASRC) of audio signals currently receives a lot of new attention due to its potential for aligning autonomous recording clients in ad-hoc acoustic sensor networks. State-of-the-art for digital-to-digital ASRC has been outlined in terms of a two-stage architecture comprising a) synchronous lowpass interpolation by an integer factor and b) subsequent asynchronous polynomial interpolation. While this composite ASRC achieves high resampling accuracy, its mere disadvantage is the intermediate oversampling to high rate. In our paper we thus fuse the high-rate discrete-time lowpass interpolation with a polynomial Farrow filter into a monolithic FIR filter form. We then show that decimation of the output rate effectively yields a polyphase set of Farrow filters with quasi-fixed coefficients. Simulations with broadband multitone signals confirm that the proposed low-rate monolithic ASRC achieves the same performance as the conventional composite resampling in terms of signal-to-interpolation-noise ratio. The main practical benefit of quasi-fixed coefficients of the system stands out when resampling by a small factor is desired, i.e., when the input rate almost matches the output rate – a scenario to be encountered in acoustic sensor networks.**

***Index Terms*—Asynchronous sampling rate conversion, sampling and interpolation, synchronization of ad-hoc acoustic sensor networks**

I. Introduction

A digital sampling rate conversion with rational conversion factors, as shown by many textbooks [1]–[5], cannot be utilized for signal alignment in ad-hoc sensor networks, where the autonomous clocks of different nodes generally cause arbitrary and even slowly time-varying sampling rate offset (SRO) between the observed signals [6]–[8]. In such scenarios, an arbitrary sampling rate conversion (ASRC) [3]–[5], [9] has to be used for SRO compensation. A wide-spread architecture of digital-to-digital ASRC is depicted in Fig. 1 for correction of a certain SRO [9]–[11]. This conventional ASRC structure[1] involves two stages: a) synchronous L-fold discrete-time upsampling with lowpass filtering and b) asynchronous polynomial interpolation of low order. The first stage can be implemented efficiently by a polyphase filter structure, but still requires a commutator switch that effectively invokes time-varying filter sets. The time-variability of the polynomial interpolator can be resolved by a Farrow structure (see Sec. II for references), but the processing still takes place in the oversampled domain.

Only few attempts were made to overcome those inconveniences by more efficient ASRC structures with both stages fused into a monolithic architecture. In [12]–[14], it was shown that the composite design can be framed as a *generalized* Farrow structure, where round-robin (commutator) activation of a number of precomputed conventional Farrow filter sets take place. Farrow's original time-invariant architecture [15] here is effectively seen as a special case of the time-varying *generalized* Farrow structure. Another work [16] comprehensively addresses optimization of the combined interpolation filter coefficients in order to achieve advanced resampling performance. The authors of these publications did, however, not draw an important conclusion of the monolithic architecture in Farrow form that we wish to convey in this contribution[2].

[1]Details about deriving the parameters μ_n, ν_n and Δ_n for controlling the resampling process according to a given SRO ε are provided in the appendix in Sec. VI, while the task of obtaining the SRO from asynchronous signals or other sources of information is not in the scope of this paper.

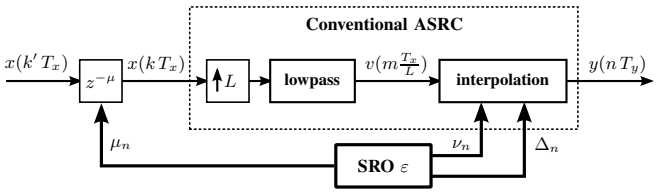

Fig. 1. Conventional composite (i.e., two-stage) ASRC based on SRO $\varepsilon = f_x/f_y - 1$, integer delay μ_n, intersample index ν_n, and fractional delay Δ_n.

We specifically look into the case where just small yet arbitrary resampling is required between the nodes in a sensor network with otherwise almost the same nominal sampling frequency [6]–[8], [17]–[20]. Hence, we require another rate decimation at the output of the time-varying Farrow structure to compensate for the intermediate expansion in the first stage. We then show that this rate decimation cancels with the polyphase commutator of the time-varying Farrow structure, unless the intersample fractional-delay time interval of the polynomial interpolation stage lapses. Our configuration therefore implies a return to almost the original and desirable time-invariant Farrow structure, while flexibility and performance of the composite architecture persist. Apart from a proof of performance, we quantitatively express the seldom change of our quasi-fixed filter sets as a function of the SRO addressed by the resampler.

This contribution is organized as follows: while the conventional composite ASRC is described in Sec. II, the proposed efficient monolithic ASRC with quasi-fixed filter coefficients is introduced in Sec. III. An experimental validation of the monolithic ASRC is presented in Sec. IV and conclusions are drawn in Sec. V. Sec. VI eventually serves as an appendix to define and illustrate computation of the control signals governed by the SRO.

II. Conventional ASRC

In digital-to-digital ASRC, FIR filters are generally preferred for interpolation because of their stability and exact linear phase [1], [9], [21]. Furthermore, a lowpass FIR filter of length N_s for synchronous L-fold upsampling, denoted by $g^{(\mathrm{s})}(m\frac{T_x}{L})$ with input sampling time T_x and oversampling-time index m, can be efficiently implemented via a polyphase decomposition resulting in a set of L corresponding polyphase FIR filters $g_\ell^{(\mathrm{s})}(kT_x)$ of length $\frac{N_s}{L}$ for $\ell \in \{0 \dots L-1\}$ [1]–[5]. On the contrary, an efficient implementation of the asynchronous interpolation, modelled usually by a continuous impulse response $g^{(\mathrm{a})}(t)$, is more challenging. An outstanding overview of the developments in interpolation theory is provided in [22].

[2]This work was supported by DFG research grant EN869/3-1 within the framework of the Research Unit FOR2457 "Acoustic Sensor Networks".

ISBN 978-90-827970-1-5 © EURASIP 2018

A. Conventional Farrow structure in the polyphase scheme

The state-of-the-art interpolators often make use of the well-known Waring-Lagrange coefficients [22]–[24], which can be calculated via explicit polynomials. A further distinctive feature of this interpolator particularly contributing to its tremendous popularity is its maximally flat frequency response at zero-frequency [25]. Thus, [26] asserts that the Waring-Lagrange filter is probably the easiest way to design asynchronous interpolators. However, the Waring-Lagrange coefficients have to be recalculated at the audio sampling rate preventing a computationally efficient implementation, which is of great significance from a practical point of view. Different attempts have been made to improve the efficiency of the interpolation, not only in time domain [27], but also in frequency domain [28]–[30]. Calculating time-variant interpolator coefficients recursively as presented in [31] is certainly another worthwhile approach. An inventive filter structure for interpolation using Waring-Lagrange coefficients with flexible polynomial order is proposed in [32] and extended to interpolation, decimation and non-uniform sampling in [33].

However, the most famous efficient architecture of asynchronous interpolation in the time domain makes use of a Farrow structure consisting of only time-invariant fixed filter coefficients [15]. It is highly attractive for real-time systems as it is fast and contains only fixed coefficients [34] and may also be implemented using the original Waring-Lagrange coefficients [35]. Since the development of the original Farrow filter, many similar design techniques have been proposed [36]–[39]. For the Farrow structure considered here, $g^{(\mathrm{a})}(t)$ is defined piecewise by polynomials of order $R-1$ in the fractional delay $\Delta_m \in [0,1)$, resulting in R subfilters $g_r^{(\mathrm{a})}(m\frac{T_x}{L})$ of length N_a for $r \in \{0 \dots R-1\}$ with fixed coefficients. The conventional ASRC with polyphase decomposition and subsequent *conventional* Farrow structure is depicted in Fig. 2. After the polyphase lowpass in the L-fold upsampled domain, the resulting signal $v(m\frac{T_x}{L})$ is delayed by $\nu_m \frac{T_x}{L}$ with $\nu_m \in \{0 \dots L-1\}$, i.e., a subsample delay w.r.t. the original sampling time interval T_x, before the Farrow filters deliver individual outputs $w_r(m\frac{T_x}{L})$. They are combined then with time-varying fractional delay Δ_m to the polynomial interpolation $\sum_{r=0}^{R-1} \Delta_m^r \, w_r(m\frac{T_x}{L})$. The L-fold decimator at the output of the system implies that the input and the final output signal will have almost the same sampling frequencies $f_x = 1/T_x$ and $f_y = 1/T_y$, up to a small SRO $\varepsilon = (f_x/f_y) - 1$ as desired by the system.

B. Generalized Farrow structure in the over-sampling scheme

Since the pioneering work of Farrow with the *conventional* Farrow structure [15], different types of Farrow structures have been proposed [40]. Exploiting a symmetry of Farrow coefficients leads to the *modified* Farrow structure resulting in further reduction of computational complexity [34]. The *generalized* Farrow structure (GFS) proposed in [12] combines the lowpass filter $g^{(\mathrm{s})}(m\frac{T_x}{L})$ with subfilters $g_r^{(\mathrm{a})}(m\frac{T_x}{L})$ of the *conventional* Farrow structure resulting in a set of R combined filters $g_r(m\frac{T_x}{L})$ of length $N = N_s + N_a - 1$ as shown in Fig. 3. Since subfilters $g_r(m\frac{T_x}{L})$ operate on the high intermediate sampling rate, an additional L-fold expander is required at the ASRC input as shown also by the conventional oversampled ASRC in Fig. 1. The subsample index $\nu_m \in \{0 \dots L-1\}$ controls R delays, which handle the integer synchronization on the expanded signal (corresponding to choosing the correct samples in a stand-alone asynchronous interpolation). The combined filters $g_r(m\frac{T_x}{L})$ consist only of fixed coefficients, hence, the system as well can be understood as an original Farrow structure in the oversampled domain. While the fixed coefficients can be designed offline before signal processing, storing the filters $g_r(m\frac{T_x}{L})$ requires more memory than storing the coefficients of $g^{(\mathrm{s})}(m\frac{T_x}{L})$ and $g_r^{(\mathrm{a})}(m\frac{T_x}{L})$ separately.

Within the signal processing community, some publications have addressed the GFS. A GFS for low-order polynomial interpolators is used in [13] and a polyphase implementation of the GFS is analytically derived in [14]. The authors of [41] argue that the GFS can be utilized for implementation of both anti-imaging and anti-aliasing lowpass filters, which is a very important feature. The *generalized modified* Farrow structure proposed in [42] combines advantages of both *modified* and *generalized* Farrow structures. An optimization method based on the GFS taking into account both synchronous and asynchronous stages of an ASRC system is developed in [16]. Further, an arbitrary sampling rate reduction can be accomplished using the *transposed* Farrow structure from [43] implemented in different ways [44]. The *prolonged* Farrow structure proposed in [45] results from prolonging the length of the polynomial segments in the Farrow structure. It should also be mentioned, that the *prolonged transposed modified* Farrow structure [46] improves the pass-band region of the *transposed* Farrow structure. Note that the subsequently proposed monolithic ASRC architecture is directly associated with the oversampled GFS as shown in Fig. 3.

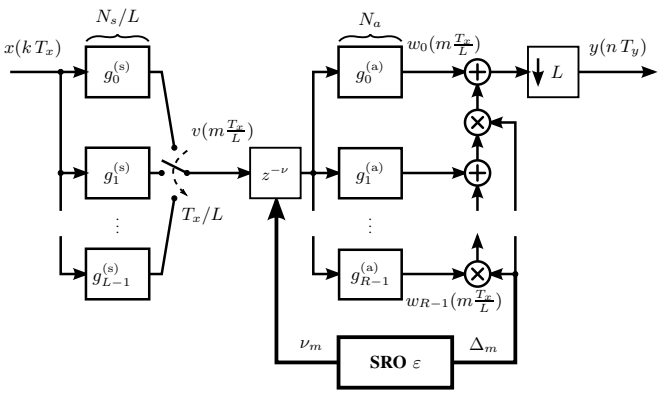

Fig. 2. Composite ASRC with polyphase decomposition and *conventional* Farrow structure: lowpass filter decomposed into L polyphase branches $g_\ell^{(\mathrm{s})}$ and Farrow structured interpolator consisting of R subfilters $g_r^{(\mathrm{a})}$.

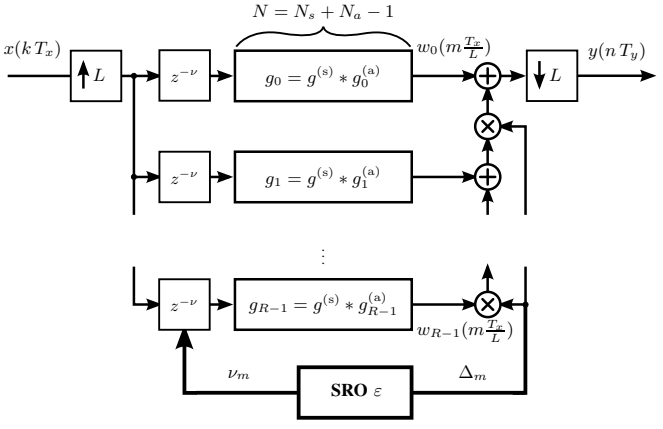

Fig. 3. ASRC in the *generalized* Farrow structure: lowpass filter $g^{(\mathrm{s})}$ combined with subfilters of Farrow structure $g_r^{(\mathrm{a})}$ via discrete-time convolution.

ISBN 978-90-827970-1-5

III. Low-rate monolithic ASRC

The motivation for developing a monolithic implementation of ASRC is strongly connected to a task at hand to align signals in an ad-hoc sensor network with similar sampling rates. Typical absolute SRO values in a wireless acoustic sensor networks could be in the range of 0-50 ppm with typical values of 10-20 ppm [6]–[8]. The proposed low-rate monolithic structure is developed in the following.

A. Generalized Farrow structure in the polyphase scheme

In a first step, we rearrange the components of the GFS shown in Fig. 3 by applying the intersample index ν to the output rather than the input of the combined filters $g_r(m\frac{T_x}{L})$. This allows the decomposition of every combined filter $g_r(m\frac{T_x}{L})$ into L polyphase filters $g_{r,\ell}(kT_x)$ of length $\frac{N}{L}$. Consequently, the L-fold expander on the input of the ASRC system is replaced by a commutating switch similar to Fig. 2. Furthermore, as preparation for the next derivation step, the final L-fold decimator in Fig. 3 is pulled into each Farrow branch. The control signals are hence calculated on the time basis of the low-rate output signal as ν_n and Δ_n (cf. Sec. VI), rather than in the upsampled domain. The resulting structure is depicted in Fig. 4. Note that N needs to be an integer multiple of L, which may be achieved via zero-padding. The advantage of this polyphase decomposition is that the combined subfilters $g_{r,\ell}(kT_x)$ become short and, even more important, work on the low input sampling rate. However, the commutator connecting the polyphase combined filters to the Farrow branch still operates on the high intermediate rate similar to the conventional ASRC approach from Fig. 2.

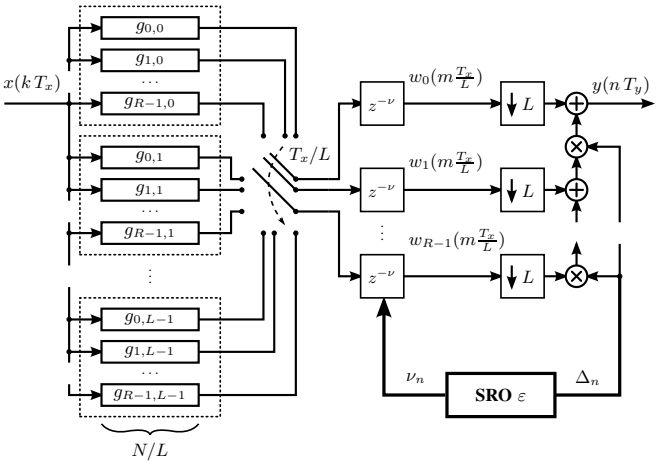

Fig. 4. Monolithic ASRC with polyphase decomposition: the commutating switch operates at a high rate of L/T_x.

B. Efficient monolithic ASRC with quasi-fixed coefficients

The final step to the proposed efficient polyphase monolithic ASRC architecture depicted in Fig. 5 is a streamlining of the signal handover between the polyphase filters and the polynomial interpolation of the ASRC system in Fig. 4. The commutator produces an intermediate high-rate digital sequence that is to be delayed via ν_n. The subsequent decimator then discards $L-1$ out of L high-rate samples before feeding the result into the polynomial interpolation. For constant intersample index $\nu_n = \nu$, i.e., while the resampler effectively operates on the same high-rate interpolation interval, the decimator always keeps the ν-th sample from the high-rate stream, corresponding to a distinct polyphase filter set $g_{0,\nu}(kT_x)\dots g_{R-1,\nu}(kT_x)$. Hence,

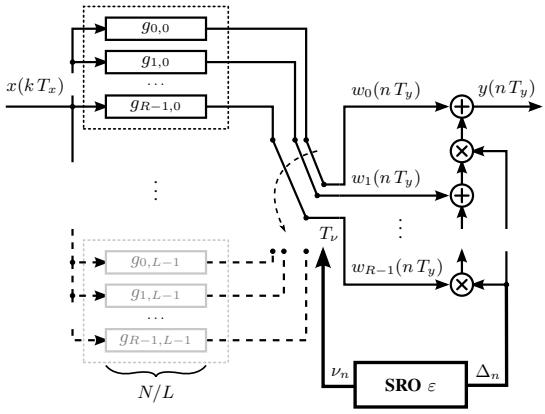

Fig. 5. Quasi-fixed monolithic ASRC: the commutator operates with a long switching interval T_ν, changing only when the fractional delay Δ_n lapses.

commutator, delays, and decimator in Fig. 4 collapse into a single commutator that switches only when ν_n changes. In applications with small SRO, that commutator thus switches very slowly, so that the filter coefficients can be viewed *quasi-fixed*. For an SRO ε defined as

$$f_x = (1+\varepsilon)\cdot f_y \tag{1}$$

with $f_x = 1/T_x$ and $f_y = 1/T_y$, the according switching interval for the intersample index ν is

$$|T_\nu| = \frac{1}{|\varepsilon|\, f_x\, L}\,. \tag{2}$$

To give an example, the commutator then switches only once every $T_\nu \approx 1.042$ s, if a nominal sampling rate of 16 kHz and an absolute SRO of 15 ppm are assumed with $L = 4$ polyphase components. For such slowly changing intersample indexes, the coefficients used in the ASRC are hence quasi-fixed. The proposed monolithic ASRC with quasi-fixed filter coefficients is thus computationally relaxed and can offer significant benefits in terms of implementation.

IV. Experimental Evaluation

The proposed monolithic ASRC architecture is evaluated in experiments with broadband discrete-multitone signals with a bandwidth $[0; f_u]$ for upper cut-off frequencies $f_u = \{2, 4, 7\}$ kHz sampled with a nominal sampling frequency of $f_y = 16$ kHz and an SRO of $\epsilon = 50$ ppm. To compensate for the SRO we compare the seven ASRC systems listed in Tab. I. The first method is an ideal Hann-windowed sinc-interpolation with support of $N_w = 513$ samples. In the second approach, the temporally closest input sample (nearest neighbour) is selected as the output without any interpolation. Both of these systems serve as an upper and lower bound of performance, respectively. All further systems rest upon polynomials with $R = 4$. The third and fourth systems are fractional-delay based ASRCs using the original Farrow filters [15] optimized for fractional delays $\Delta_m \in [0; 1)$ and normalized frequency range $\Omega \in [0; 7/8]$. Both systems hence neglect the explicit lowpass support as of Fig. 1 and Fig. 2. System 3 operates with $N_a = 4$ coefficients, while best possible performance according to our experiments is achieved with $N_a = 48$ coefficients in system 4. The remaining three ASRC systems in Tab. I are based on the support of both, a discrete-time lowpass interpolation ($L = 8$) in the first stage and a Waring-Lagrange interpolation ($N_a = R$) in the second stage, while the precise implementation is according to Fig. 2, Fig. 3 and Fig. 5,

ISBN 978-90-827970-1-5

TABLE I
PERFORMANCE AND PROPERTIES OF DIFFERENT ASRC SYSTEMS.

	SINR / dB					
	$f_u = 2\,\text{kHz}$	$f_u = 4\,\text{kHz}$	$f_u = 7\,\text{kHz}$	lowpass filter	low-rate processing	fixed coefficients
1. Win-Sinc ($N_w = 513$)	107.5	107.3	107.3		✓	
2. Nearest neighbor	17.7	11.7	7.0		✓	
3. Farrow ($N_a = 4$)	24.7	23.0	18.5		✓	✓
4. Farrow ($N_a = 48$)	88.1	64.0	45.1		✓	✓
5. Composite (Fig. 2)	98.2	96.4	82.1	✓		
6. Generalized (Fig. 3)	98.2	96.4	82.1	✓		✓
7. Low-rate (Fig. 5)	98.2	96.4	82.1	✓	✓	✓

respectively. The lowpass filter is designed using the Parks-McClellan method for $N_s = 797$ with a passband cutoff frequency $f_p = 7\,\text{kHz}$ and a stopband cutoff frequency $f_s = 8\,\text{kHz}$ [47].

The performance of the ASRC systems is evaluated in terms of signal-to-interpolation-noise ratio (SINR) listed in Tab. I. We observe that the system performance naturally decays with increasing bandwidth f_u. Application of the lowpass filter in systems 5–7 causes a performance gain of 10–37 dB compared to the landmark system 4. The system 7 achieves the same performance as systems 5 and 6 in terms of SINR, proving the equivalence of the proposed approach with the conventional ASRC. The monolithic ASRC with quasi-fixed coefficients is, however, set apart from systems 5 and 6 by the desired low-rate processing in Tab. I. The proposed system thus combines the low-rate processing of systems 1–4 with the lowpass filtering of systems 5 and 6 while maintaining fixed coefficients.

To further demonstrate flexibility and performance of the proposed monolithic ASRC for different values of parameters $N = N_s + N_a - 1$ and L, further experiments are carried out using multitone signals with $f_u = 7\,\text{kHz}$. Waring-Lagrange coefficients for $R = N_a = 4$ are still used for asynchronous interpolation. As shown in Fig. 6, the system performance measured in terms of SINR steadily improves with increasing length N_s of the lowpass filter until saturation due to the limitation of polynomial interpolation. The resampling

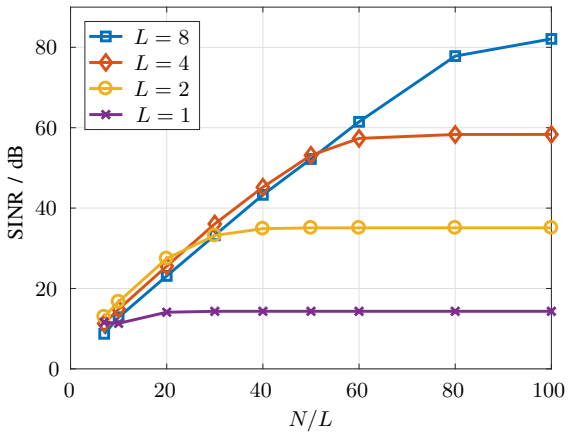

Fig. 6. Performance of low-rate monolithic ASRC from Fig. 5 with Waring-Lagrange interpolation ($R = N_a = 4$) and different lowpass parameters.

performance further increases here with the choice of the implicit discrete-time lowpass upsampling factor L, where $L = 1$ effectively corresponds to just Waring-Lagrange interpolation.

V. CONCLUSION

In this contribution, an efficient monolithic ASRC architecture has been derived for aligning the discrete-time signals with almost the same nominal sampling frequency – a scenario often encountered in ad-hoc acoustic sensor networks. Retaining the same high resampling performance as the conventional composite ASRC approach, the proposed structure can be implemented as a monolithic filter structure with quasi-fixed coefficients. For small SROs, the filter sets only need to change seldom, making the proposed approach suitable for future block-based frequency domain implementation. The proposed structure does, however, not yet exploit the symmetry of the filter coefficients, which can be addressed in further developments.

VI. APPENDIX

For an illustration of how the control signals in Fig. 1 $\mu_n \in \mathbb{Z}$, $\nu_n \in \{0, 1, \ldots, L-1\}$ and $\Delta_n \in [0; 1)$ are calculated for a given SRO, for instance $\varepsilon = \frac{1}{3}$ according to (1), the original sampling times of signal $x(k' T_x)$ and the desired sampling times of signal $y(n T_y)$ (cf. Fig. 1) are depicted in Fig. 7 as red circles and green crosses, respectively. In this timing diagram, a perfect synchronization is assumed in the beginning of the resampling process and the samples added by the L-folded expander are depicted as blue empty circles.

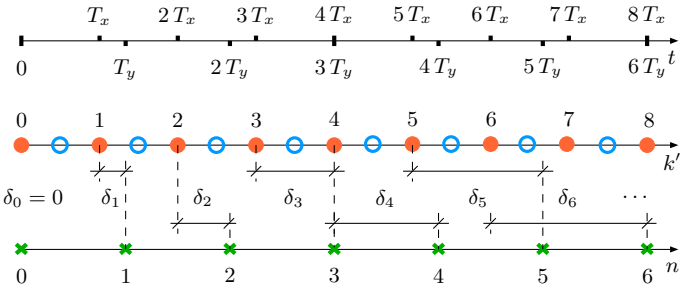

Fig. 7. Timing diagram for $\varepsilon = \frac{1}{3}$ and $L = 2$.

The sampling times of $y(n T_y)$ counted with $n \in \mathbb{Z}$ correspond to the real-valued sampling times $\kappa_n = n + \delta_n \in \mathbb{R}$ on the k'-axis with an accumulating time drift $\delta_n = \varepsilon \cdot n$. Thus, the values of μ_n, ν_n and Δ_n are calculated from δ_n as follows:

$$\mu_n = \lfloor \delta_n \rfloor, \quad \nu_n = \lfloor L \cdot \{\delta_n\} \rfloor, \quad \Delta_n = \{L \cdot \{\delta_n\}\}, \qquad (3)$$

where $\lfloor \cdot \rfloor$ and $\{\cdot\}$ are the common floor and fractional part functions, respectively. The values μ_n, ν_n, and Δ_n for the example in Fig. 7 are calculated with (3) and given in Tab. II to complete the illustration.

TABLE II
THE VALUES OF μ_n, ν_n AND Δ_n FROM FIG. 7 CALCULATED WITH (3).

n	κ_n	δ_n	μ_n	ν_n	Δ_n
1	$1\frac{1}{3}$	$\frac{1}{3}$	0	0	$\frac{2}{3}$
2	$2\frac{2}{3}$	$\frac{2}{3}$	0	1	$\frac{1}{3}$
3	4	1	1	0	0
4	$5\frac{1}{3}$	$1\frac{1}{3}$	1	0	$\frac{2}{3}$
5	$6\frac{2}{3}$	$1\frac{2}{3}$	1	1	$\frac{1}{3}$
6	8	2	2	0	0

Note, Δ_n is calculated as fractional part of the time interval T_x/L.

ISBN 978-90-827970-1-5 © EURASIP 2018

REFERENCES

[1] R. E. Crochiere and L. R. Rabiner, *Multirate Digital Signal Processing*, Prentice Hall, 1983.

[2] P. P. Vaidyanathan, *Multirate Systems and Filter Banks*, Pearson Education India, 1993.

[3] J. G. Proakis and D. G. Manolakis, *Digital Signal Processing: Principles, Algorithms and Applications (3. ed.)*, Prentice-Hall Int. Corp., 1996.

[4] H. G. Göckler and A. Groth, *Multiratensysteme: Abtastratenumsetzung und digitale Filterbänke*, Schlembach, 2004.

[5] P. Prandoni and M. Vetterli, *Signal Processing for Communications*, EPFL Press, 2008.

[6] J. R. Vig, "Introduction to quartz frequency standards. Research and development technical report SLCET-TR-92-1 (rev. 1)," Tech. Rep., Army Research Laboratory, Electronics and Power Sources Directorate, Oct. 1992.

[7] Y.-C. Wu, Q. Chaudhari, and E. Serpedin, "Clock synchronization of wireless sensor networks," *IEEE Signal Processing Magazine*, vol. 28, no. 1, pp. 124–138, Jan. 2011.

[8] D. Cherkassky and S. Gannot, "Blind synchronization in wireless acoustic sensor networks," *IEEE Transactions on Audio, Speech, and Language Processing*, vol. 25, no. 3, pp. 651–661, Mar. 2017.

[9] G. Evangelista, *Zum Entwurf digitaler Systeme zur asynchronen Abtastratenumsetzung*, Ph.D. thesis, Ruhr-Universität Bochum, 2001.

[10] T. A. Ramstad, "Digital methods for conversion between arbitrary sampling frequencies," *IEEE Transactions on Acoustic, Speech, and Signal Processing*, vol. 32, no. 3, pp. 577–591, June 1984.

[11] T. Saramaki and T. Ritoniemi, "An efficient approach for conversion between arbitrary sampling frequencies," in *Proc. of IEEE International Symposium on Circuits and Systems*, May 1996, vol. 2, pp. 285–288.

[12] T. A. Ramstad, "Fractional rate decimator and interpolator design," in *European Signal Processing Conference (EUSIPCO)*, Sept. 1998, pp. 1–4.

[13] L. Lundheim and T. A. Ramstad, "An efficient and flexible structure for decimation and sample rate adaptation in software radio receivers," in *Proc. ACTS Mobile Communications Summit*, June 1999.

[14] T. A Ramstad, "Flexible and efficient interpolator design," in *Proc. of Norwegian Signal Processing Symposium (NORSIG)*, Sept. 1999.

[15] C. W. Farrow, "A continuously variable digital delay element," in *Proc. of IEEE International Symposium on Circuits and Systems*, June 1988, pp. 2641–2645.

[16] A. Franck, *Efficient algorithms for arbitrary sample rate conversion with application to wave field synthesis*, Ph.D. thesis, Technische Universität Ilmenau, 2012.

[17] J. Schmalenstroeer, P. Jebramcik, and R. Haeb-Umbach, "A combined hardware-software approach for acoustic sensor network synchronization," *Signal Processing, Elsevier*, vol. 107, pp. 171 – 184, 2015.

[18] L. Wang and S. Doclo, "Correlation maximization-based sampling rate offset estimation for distributed microphone arrays," *IEEE/ACM Transactions on Audio, Speech, and Language Processing*, vol. 24, no. 3, pp. 571–582, Mar. 2016.

[19] M. H. Bahari, A. Bertrand, and M. Moonen, "Blind sampling rate offset estimation for wireless acoustic sensor networks through weighted least-squares coherence drift estimation," *IEEE/ACM Transactions on Audio, Speech and Language Processing (TASLP)*, vol. 25, no. 3, pp. 674–686, Mar. 2017.

[20] J. Schmalenstroeer, J. Heymann, L. Drude, C. Boeddecker, and R. Haeb-Umbach, "Multi-stage coherence drift based sampling rate synchronization for acoustic beamforming," in *Proc. of IEEE International Workshop on Multimedia Signal Processing (MMSP)*, Oct. 2017, pp. 1–6.

[21] R. W. Schafer and L. R. Rabiner, "A digital signal processing approach to interpolation," *Proc. of the IEEE*, vol. 61, no. 6, pp. 692–702, June 1973.

[22] E. Meijering, "A chronology of interpolation: From ancient astronomy to modern signal and image processing," *Proc. of the IEEE*, vol. 90, no. 3, pp. 319–342, May 2002.

[23] E. Waring, "Problems concerning interpolations," *Philosophical Transactions of the Royal Society of London*, vol. 69, pp. 59–67, Jan. 1779.

[24] J. L. Lagrange, "Leçons élémentaires sur les mathématiques données à l'école normale en 1795," in *Œuvres complètes*, vol. 7, pp. 183–287. Paris, France: Gauthier-Villars, 1877.

[25] G. Oetken, "A new approach for the design of digital interpolating filters," *IEEE Transactions on Acoustics, Speech, and Signal Processing*, vol. 27, no. 6, pp. 637–643, Dec. 1979.

[26] T. I. Laakso, V. Valimäki, M. Karjalainen, and U. K. Laine, "Splitting the unit delay," *IEEE Signal Processing Magazine*, vol. 13, no. 1, pp. 30–60, Jan. 1996.

[27] G. Evangelista, "Design of digital systems for arbitrary sampling rate conversion," *Signal Processing*, vol. 83, no. 2, pp. 377–387, Feb. 2003.

[28] G. Bi and S. K. Mitra, "Sampling rate conversion in the frequency domain," *IEEE Signal Processing Magazine*, vol. 28, no. 3, pp. 140–144, May 2011.

[29] S. Miyabe, N. Ono, and S. Makino, "Blind compensation of interchannel sampling frequency mismatch for ad hoc microphone array based on maximum likelihood estimation," *Signal Processing, Elsevier*, vol. 107, pp. 185 – 196, Sept. 2015.

[30] J. Schmalenstroeer and R. Haeb-Umbach, "Efficient sampling rate offset compensation - an Overlap-Save based approach," in *Proc. of European Signal Processing Conference (EUSIPCO)*, Sept. 2018.

[31] A. I. Russell and P. E. Beckmann, "Efficient arbitrary sampling rate conversion with recursive calculation of coefficients," *IEEE Transactions on Signal Processing*, vol. 50, no. 4, pp. 854–865, Apr. 2002.

[32] C. Candan, "An Efficient Filtering Structure for Lagrange Interpolation," *IEEE Signal Processing Letters*, vol. 14, no. 1, pp. 17–19, Jan. 2007.

[33] V. Lehtinen and M. Renfors, "Structures for interpolation, decimation, and nonuniform sampling based on Newton's interpolation formula," in *International Conference on Sampling Theory and Applications*, May 2009.

[34] J. Vesma and T. Saramaki, "Interpolation filters with arbitrary frequency response for all-digital receivers," in *Proc. of IEEE International Symposium on Circuits and Systems*, May 1996, vol. 2, pp. 568–571.

[35] V. Valimäki, "A new filter implementation strategy for Lagrange interpolation," in *Proc. of IEEE International Symposium on Circuits and Systems*, Apr. 1995, vol. 1, pp. 361–364.

[36] G. D. Cain, A. Yardim, and P. Henry, "Offset windowing for FIR fractional-sample delay," in *Proc. of International Conference on Acoustics, Speech, and Signal Processing*, May 1995, vol. 2, pp. 1276–1279.

[37] F. Harris, "Performance and design of Farrow filter used for arbitrary resampling," in *Proc. of 13th International Conference on Digital Signal Processing*, July 1997, vol. 2, pp. 595–599, vol. 2.

[38] V. Valimäki and T. I. Laakso, "Principles of fractional delay filters," in *Proc. of IEEE International Conference on Acoustics, Speech, and Signal Processing*, June 2000, vol. 6, pp. 3870–3873.

[39] Marek Blok, "Fractional delay filter design for sample rate conversion," in *Proc. of Federated Conference on Computer Science and Information Systems (FedCSIS)*, Sept. 2012, pp. 701–706.

[40] F. M. Klingler and H. G. Göckler, "Conversion between arbitrary sampling rates: an implementation cost trade-off study for the family of Farrow structures," in *Proc. of Karlsruhe Workshop on Software Radios*, Mar. 2008.

[41] T. Hentschel, *Sample rate conversion in software configurable radios*, Artech House, 2002.

[42] M. T. Hunter and W. B. Mikhael, "A novel Farrow structure with reduced complexity," in *in Proc. of IEEE International Midwest Symposium on Circuits and Systems*, 2009, pp. 581–585.

[43] T. Hentschel and G. Fettweis, "Continuous-time digital filters for sample-rate conversion in reconfigurable radio terminals," *Frequenz*, vol. 55, no. 5-6, pp. 185–188, 2001.

[44] D. Babic, J. Vesma, T. Saramaki, and M. Renfors, "Implementation of the transposed Farrow structure," in *Proc. of IEEE International Symposium on Circuits and Systems*, 2002, vol. 4, pp. 5–8.

[45] D. Babic, T. Saramäki, and M. Renfors, "Conversion between arbitrary sampling rates using polynomial-based interpolation filters," in *Proc. of International TICSP Workshop on Spectral Methods and Multirate Signal Processing*, Sept. 2002, pp. 57–64.

[46] D. Babic, T. Saramaki, and M. Renfors, "Prolonged transposed polynomial-based filters for decimation," in *Proc. of International Symposium on Circuits and Systems*, May 2003, vol. 4, pp. IV–317–IV–320.

[47] Digital Signal Processing Committee of the IEEE Acoustics, Speech, and Signal Processing Society, Ed., *Programs for Digital Signal Processing*, IEEE Press, New York, 1979, Algorithm 5.1.

ISBN 978-90-827970-1-5 © EURASIP 2018